Fluid Temperature Measurement in Aqueous Solution via Electrochemical Impedance

Alex Baldwin, Eugene Yoon, Trevor Hudson, and Ellis Meng, *Fellow, IEEE*

***Abstract*— A novel temperature transduction method using the high-frequency electrochemical impedance between a pair of microelectrodes exposed to aqueous solution is reported. The solution resistance of an aqueous ionic solution is highly temperature dependent, and the electrochemical impedance between two microelectrodes is dominated by solution resistance when measured at the appropriate frequency. Therefore, precise measurements of electrochemical impedance at the proper frequency in a two-electrode system can be used to transduce solution temperature. To demonstrate this method, a temperature sensor composed of two thin-film platinum electrodes on a freestanding Parylene C substrate was designed and fabricated. A platinum resistance temperature detector was co-fabricated to provide a simple means of benchmarking against an existing standard. Transduction via electrochemical impedance was achieved by measuring the real part of impedance at the frequency where phase was minimized. Fluid temperature was transduced between 15°C and 50°C with high sensitivity (−1.21%/°C) and resolution (0.02°C). A 4× improvement in sensitivity and resolution over the conventional platinum resistance temperature detector was achieved. The sensor design described here features flexible construction with inert materials which facilitates future use in biomedical or microfluidic applications. [2019-0190]**

***Index Terms*— Temperature measurement, electrochemical impedance, biomedical sensor, thin film sensor, flexible sensor.**

I. Introduction

TEMPERATURE measurement of aqueous solutions is vital in a number of different microfluidic, medical, and biological applications. To measure flow rate, precise temperature measurement can be utilized to create a thermal flow sensor which tracks heat flow due to the moving liquid [1]. Applications of thermal liquid flow sensors include flow cytometry [2], drug delivery dosing [3], and lab-on-chip devices [4], [5]. In the medical realm, precise temperature measurement in the body can be used to monitor blood perfusion to an organ [6] or as part of a control system to avoid these pathological states [7], [8]. Many of these applications involve prolonged exposure to saline or other aqueous ionic liquids; therefore, a temperature sensing method that can withstand a corrosive saline environment is desirable.

State-of-the-art methods for fluid temperature measurement include thermocouples and resistance temperature detectors (RTDs) [9], [10]. Thermocouples utilize the Seebeck effect, in which a temperature-dependent voltage occurs at the junction of two dissimilar conducting elements [11]. They are generally constructed from nickel alloys and have temperature sensitivities up to 60 μV/°C, though their precision is low (±2°C). Semiconductor junctions can also be used as thermocouples, with sensitivities up to 110 mV/°C and precisions approaching ±0.8°C [9]. However, thermocouples require encapsulation to protect conducting elements from water intrusion or shield the body from non-biocompatible materials, further reducing sensitivity.

RTDs are conductive or semiconductive elements whose resistance changes with temperature. Most metal RTDs use platinum due to its highly linear response, but other metals such as copper and nickel can be used as well. The standard PT100 RTD is made of bulk platinum wire and defined by a resistance of 100 Ω at 0°C [10]. Platinum RTDs can also be microfabricated on thin-film substrates, though the temperature sensitivity of thin-film platinum (0.198%/°C for ∼100 nm films) is lower than in bulk platinum (0.385%/°C) [12]. Laboratory-grade RTDs can operate between −200 and 1000°C with precision approaching ±0.001°C whereas commercial RTDs can have precisions on the order of ±0.03°C. Drawbacks of platinum RTDs include low sensitivity and the requirement for encapsulation in aqueous solutions, to prevent unwanted charge transfer through the solution and biofouling. Semiconductor RTDs are known as thermistors, and can possess temperature coefficients of resistance approaching −2%/°C [9], [13]. However, semiconductors corrode and disintegrate during chronic soaking in aqueous solutions [14]–[16].

This work proposes an alternate method of fluid temperature transduction via direct measurement of a fluid's solution resistance. The solution resistance between electrodes immersed in an aqueous ionic solution is highly sensitive to temperature changes, mainly due to decreases in water's viscosity with increased temperature. Decreasing viscosity increases the mobility of ions dissolved in solution, which lowers a solution's electrical resistivity. The temperature sensitivity of an aqueous solution's resistivity matches or exceeds

Manuscript received August 26, 2019; accepted September 3, 2019. Date of publication September 18, 2019; date of current version December 4, 2019. This work was supported in part by the U.S. National Science Foundation under Award EFRI-1332394 and in part by the Alfred E. Mann Institute Fellowship (AB). Subject Editor Y. Zohar. *(Corresponding author: Alex Baldwin.)*

A. Baldwin is with Niche Biomedical Inc., Los Angeles, CA 90024 USA (e-mail: axbaldwin@gmail.com).

E. Yoon and T. Hudson are with the Department of Biomedical Engineering, University of Southern California, Los Angeles, CA 90089 USA (e-mail: eugenejy@usc.edu; tqhudson@usc.edu).

E. Meng is with the Department of Biomedical Engineering, University of Southern California, Los Angeles, CA 90089 USA, and also with the Ming Hsieh Department of Electrical and Computer Engineering, University of Southern California, Los Angeles, CA 90089 USA (e-mail: ellis.meng@usc.edu).

Color versions of one or more of the figures in this article are available online at http://ieeexplore.ieee.org.

Digital Object Identifier 10.1109/JMEMS.2019.2939811

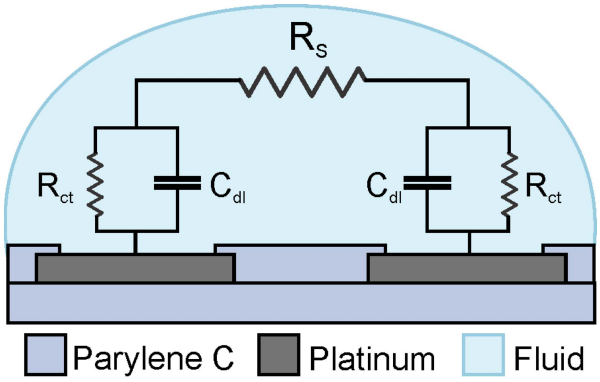

Fig. 1. Temperature sensors are composed of 2000 Å thick platinum electrodes (exposed area 150 × 250 μm^2) sandwiched between 10 μm thick layers of Parylene C and exposed to the solution. The electrochemical impedance between two identical electrodes consists of the solution resistance R_S, as well as a charge transfer resistance R_{ct} and double layer capacitance C_{dl} at each electrode interface. At high measurement frequencies, the double layer capacitance acts as a short circuit and impedance can be approximated as R_S.

the sensitivities of semiconductor materials; for example, the reported temperature coefficient of resistivity for human cerebrospinal fluid at body temperature was previously measured as −1.98%/°C [17]. It follows that measuring solution resistance using high-frequency electrochemical impedance enables highly sensitive fluid temperature transduction.

Low-frequency electrochemical impedance was measured across the terminals of a lithium-ion battery to transduce its internal temperature [18], [19]. The temperature transduction method was based on charge transfer resistance and not investigated for other applications. In contrast, this work utilizes the temperature sensitivity of high frequency electrochemical impedance measured between two microfabricated electrodes exposed to saline and demonstrates precise temperature transduction. Previously, qualitative measurement of high frequency electrochemical impedance using microfabricated platinum electrodes was used to create a thermal flow sensor [20], [21]. Impedance measurements were used to track the time of flight of a heat pulse, allowing for measurement of low flow rates with minimal overheat temperature. The present temperature detector builds off this early qualitative demonstration for flow measurement. In comparison to earlier methods relying on charge transfer resistance, potential toxic byproducts of Faradaic reactions are avoided, and rapid measurement is possible.

II. Theory

The electrochemical impedance between two identical electrodes immersed in solution can be approximated as a simplified Randles circuit [22] which includes a charge transfer resistance R_{ct} and double layer capacitance C_{dl} at each electrode-electrolyte interface, and the solution resistance R_s between electrodes (Fig. 1).

R_{ct} describes charge transfer between the metal electrode and the aqueous solution due to Faradaic redox reactions. For a given overpotential v_0, the net current i_{net} is given by:

$$i_{net} = i_o \left\{ \frac{C_o(0,t)}{C_o^*} e^{-v_0 \alpha_c nF/RT} - \frac{C_R(0,t)}{C_R^*} e^{v_0(1-\alpha_c)nF/RT} \right\} \quad (1)$$

where $C_O(0,t)$ or $C_R(0,t)$ is the concentration of the oxidized or reduced species at 0 displacement from the electrode at time = t, C_O^* or C_R^* is the bulk concentration of the oxidized or reduced species, α_c is a transfer coefficient which can range from zero to unity, n is number of electrons transferred, i_0 is the exchange current density, F is Faraday's constant, R is the gas constant, and T is temperature in Kelvin [23], [24]. Using the linear approximation of an exponential ($e^x \approx 1 + x$), this equation can be simplified to give an expression for charge transfer resistance in response to small overpotentials:

$$i_{net} = \frac{-i_o nF}{RT} v_0 \quad (2)$$

$$R_{ct} = \frac{dv_0}{di_{net}} = \frac{RT}{nFi_o} \quad (3)$$

Equation 3 implies a direct correlation between R_{ct} and temperature. However, the byproducts of Faradaic reactions can be toxic [25], so measurement of R_{ct} in biological or microfluidic systems is undesirable. Furthermore, R_{ct} only factors in to the impedance of microelectrodes at frequencies <1 Hz [26], preventing rapid measurement which limits the utility of the technique. Therefore, practical electrochemical impedance measurements between microelectrodes directly exposed to solution will be composed of C_{dl} and/or R_S.

The capacitance C_{dl} is created by the double layer of electrostatically-bound ions that builds up at the electrode-electrolyte interface [27]. Helmholtz, Gouy-Chapman, Stern, Graham, and others have modeled this phenomenon, but the precise relationships between C_{dl} and temperature remains an area of ongoing research [28], [29].

Solution resistance, R_S, is highly sensitive to changes in temperature. The solution resistance between two electrodes depends on the orientation of and distance between electrodes, but generalized expressions can be developed by considering an electrolyte solution's resistivity or its reciprocal value, conductivity. Bulk conductivity is proportional to ionic concentration, but a molar conductivity $\Lambda = G/c$ can be defined, where G is bulk conductance and c is concentration [30]. As ionic concentration goes to zero, interionic forces disappear. This is known as the state of infinite dilution and can be modeled using Stoke's law as:

$$\lambda_0 = \frac{qF}{4\pi\eta r} \quad (4)$$

where λ_0 is conductivity at infinite dilution, q is ionic charge, η is water's viscosity, and r is ionic radius [31]. Only viscosity varies significantly with temperature; therefore, the temperature coefficient of solution resistance at infinite dilution is proportional to water's viscosity [20].

At concentrations above infinite dilution, solution conductivity will decrease. Interionic forces at concentrations above infinite dilution can be modeled using Debye-Huckel-Onsager theory [32]; the Kohlrausch equation can then be employed to generate the following expression for solution conductivity:

$$\Lambda = \lambda^0 - \left(\frac{z^2 eF^2}{3\pi\eta\sqrt{\frac{2}{\varepsilon_0 RT}}} + \frac{xz^3 eF}{24\pi\varepsilon_0 RT\sqrt{\frac{2}{\varepsilon RT}}} \lambda^0 \right) \sqrt{c} \quad (5)$$

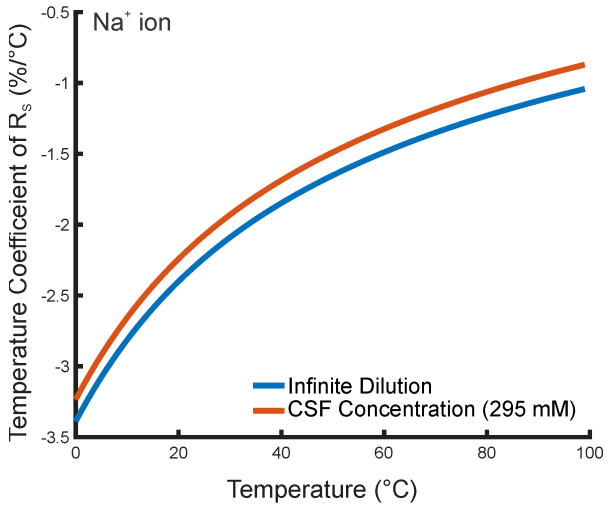

Fig. 2. The temperature coefficient of solution resistance for a solution of sodium ions at infinite dilution and at the osmolarity of cerebrospinal fluid (CSF). At infinite dilution, the temperature coefficient ranges from −3.39%/°C at 0°C to −1.04%/°C at 100°C, with a value of −1.91%/°C at body temperature (37°C). Increasing ionic concentration decreases temperature sensitivity; at the osmolarity of CSF (295 mOsm), the temperature coefficient of solution resistance decreases to −1.75%/°C at body temperature. Figure generated via MATLAB.

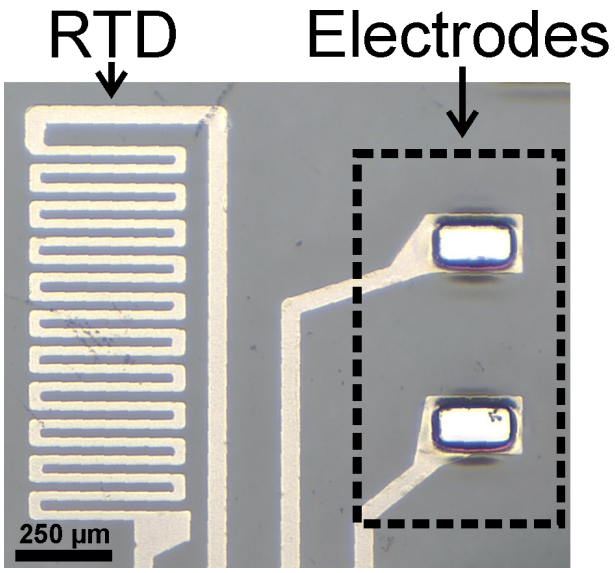

Fig. 3. Impedimetric temperature sensing was tested using a pair of platinum electrodes on a Parylene C substrate. A microfabricated platinum RTD on the same substrate was used for benchmarking.

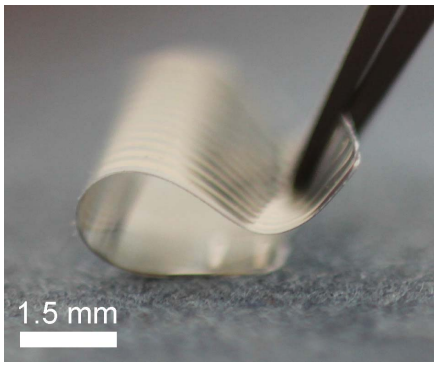

Fig. 4. Fabrication on a Parylene C substrate give sensors flexibility, enabling simple packaging and integration into catheters and shunts used in the clinic.

where c is electrolyte concentration in moles per liter, z is the valency number of each ionic species, e is the electron charge, and x describes ionic symmetry [33].

This expression for solution conductivity can be used to calculate the sensitivity of solution resistance to temperature. Empirical measurements for the viscosity [34], permittivity [22], and Debye relaxation time [23] of pure water and the hydrated radius of a sodium ion [35] were used to calculate temperature coefficients of solution resistance of a solution of sodium ions (Fig. 2). At infinite dilution, the temperature coefficient of resistance calculated using Equation 5 ranged from −3.39%/°C at 0°C to −1.04 %/°C at 100°C. Equation 6 can be used to calculate the temperature coefficient of solution resistance at concentrations above infinite dilution; temperature sensitivity decreases at higher concentrations compared to infinite dilution, but there is minimal change in temperature coefficient between 100 mOsm and 1 Osm. At body temperature (37°C), the temperature coefficient of solution resistance is −1.75%/°C at a typical osmolarity of cerebrospinal fluid (295 mOsm [36]), compared to −1.91%/°C at infinite dilution.

The predictable and highly sensitive relationship between R_S and temperature suggests a possible method for temperature transduction. By measuring electrochemical impedance at high frequencies where phase is minimized, C_{dl} and R_{ct} are rendered negligible and impedance consists only of R_S. Therefore, fluid temperature can be transduced using high-frequency electrochemical impedance.

III. Design and Fabrication

A temperature sensor was designed and fabricated to transduce fluidic temperature via high-frequency impedance. The sensor consisted of a pair of platinum electrodes on a Parylene C substrate (Fig. 3). Electrodes had exposed areas $150 \times 250\ \mu m^2$ with centers 750 μm apart. A platinum resistor, placed 1 mm away from the electrodes on the same Parylene C substrate, was used as an RTD for benchmarking. This RTD consisted of a serpentine trace 25 μm wide with nominal DC resistance of ∼450 Ω. Construction out of platinum on a Parylene C substrate leaves sensors flexible, [37] (Fig. 4) for simpler integration into microfluidic packaging. In addition, both Parylene C and platinum are non-toxic and have a long history of use in chronically implantable medical devices [38], [39].

Devices were fabricated using previously-reported polymer micromachining techniques [40], [41]. First, a 10 μm thick layer of Parylene C was deposited onto a 4" silicon carrier wafer using a SCS LabCoter 2 chemical vapor deposition system (Specialty Coating Systems, Indianapolis, IN, USA). Next, a mask for metal deposition composed of 2 μm thick AZ 5214 photoresist (Integrated Micro Materials, Argyle, TX, USA), was spin-coated and patterned using UV lithography. A 2000 Å thick layer of platinum was electron-beam deposited

and patterned via liftoff. A second 10 μm thick layer of Parylene C was deposited as insulation, then electrodes and contact pads were defined by a switched-chemistry deep reactive ion etch in oxygen plasma [41] using an Oxford Plasmalab 100 inductively coupled plasma etcher (Oxford Instruments, Abington, UK). For oxygen plasma etching, an etch mask was defined using a 15 μm thick layer of AZ P4620 photoresist (Integrated Micro Materials, Argyle, TX, USA). Devices were released from the carrier wafer by gently peeling while immersed in deionized water, then cleaned by soaking in acetone, isopropyl alcohol, and deionized water for ten minutes each. After release, devices were thermally annealed at 200°C for 48 hours in a vacuum environment; thermal annealing increases crystallinity, decreasing flexibility slightly but improving adhesion between adjacent Parylene C layers [40], [42]–[45].

Electrical connection to devices was achieved by attaching a 250 μm thick PEEK (polyetheretherketone) backing to contact pads using cyanoacrylate glue and inserting into a zero insertion force connector [46] (ZIF; Hirose Electric Co. Ltd., Tokyo, Japan). Electrical connections were protected during soaking using EpoTek 353ND-T epoxy (Epoxy Technology Inc., Billerica, MA, USA).

IV. Testing Methods

Sensors were primarily tested in phosphate-buffered saline (1× PBS), a common physiological fluid analog. 1× PBS is similar in composition to cerebrospinal fluid and possesses a nominal resistivity of 50 Ω·cm. For comparison, the conductivity of human cerebrospinal fluid has been measured as 68.7±1.1 Ω·cm at room temperature and 55.5±0.7 Ω·cm at body temperature [17]. Transduction was also evaluated in concentrated PBS (10×PBS, resistivity 5 Ω·cm) and deionized (DI) water (resistivity 18 MΩ·cm).

For electrochemical impedance spectroscopy (EIS), sensors were sealed in glass vials filled with 1× PBS and placed in a water bath, which was heated to temperatures between 30 and 50°C. A Gamry Reference 600 potentiostat was used for EIS measurement. For single-frequency impedance tests, solution was heated from room temperature (∼20°C) to 50°C using a hot plate or cooled to 15°C with ice packs. A thermocouple/multimeter (Newport TrueRMS Supermeter, ±2°C accuracy) was used to monitor fluid temperature and calibrate the co-fabricated RTD; RTD calibration was achieved by comparing resistance measurements to thermocouple data over multiple cycles and generating a linear regression. Data was collected from impedance electrodes using an Agilent E4980A precision LCR meter with a measurement amplitude of 0.1 V_{PP}, to stay within the low overpotential regime. Data was acquired from the RTD using a Keithley SourceMeter with 10 μA bias current. The impedance between electrodes and the resistance of the platinum RTD were simultaneously collected and analyzed using LabVIEW.

To evaluate drift, a sensor die was sealed into a silicone tube using EpoTEK 353-NDT epoxy and exposed to room temperature 1× PBS for 24 hours. Fluid was flowed past the sensor at 100 μL/min using a Watson-Marlow 120U peristaltic pump to prevent local variations in the bulk ionic concentration. Impedance and RTD resistance were recorded once per minute, and a Sensirion SLI-1000 operating in its temperature transduction mode (±0.1°C precision) was used to confirm measurements.

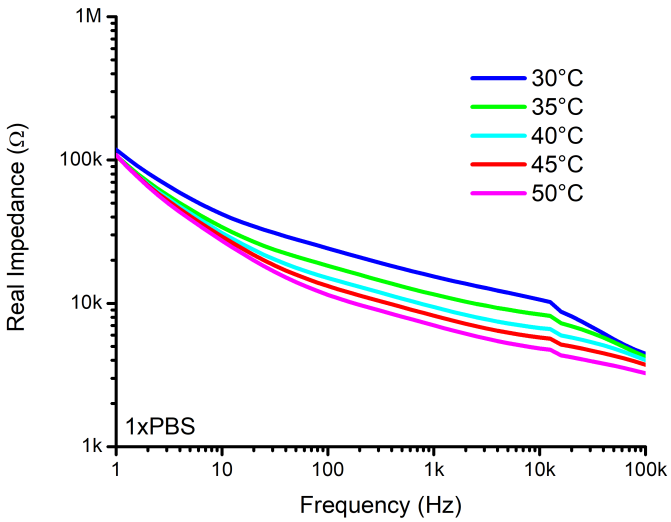

Fig. 5. Electrochemical impedance spectroscopy between two platinum electrodes at temperatures between 30 and 50°C. As temperature increased, the real impedance at high frequencies decreased.

V. Experimental Results

EIS from 1 Hz to 100 kHz was performed at 5°C temperature intervals from 30 to 50°C (Fig. 5). Only the real part of impedance was recorded in order to remove any interference from parasitic capacitances. Results showed a clear temperature dependency of impedance at high frequencies.

The platinum RTD was calibrated by comparing its resistance to thermocouple measurements in 1×PBS, revealing a temperature coefficient of resistance of 1.21 Ω/°C. Temperature was then cycled between 20 and 50°C while simultaneously measuring the impedance across the electrodes at 100 kHz, the DC resistance of the RTD, and fluid temperature from the thermocouple. The real part of impedance correlated with temperature with a sensitivity of -58.29 Ω/°C (Fig. 6). The resolution, calculated as 3× the average RMS noise across the tested temperature range divided by the linearized temperature coefficient of resistance between 20 and 50°C, was 0.02°C for impedance-based temperature sensing and 0.08°C for the platinum RTD. Direct comparison between temperature measurements using the calibrated RTD and real impedance values exhibited an inverse relationship (Fig. 7). Minimal hysteresis was observed over 8 cycles. Both electrode impedance and RTD resistance responded to ±30°C changes in temperature in less than 200 ms.

Temperature sensing was then evaluated in DI water and 10× PBS. First, EIS between the microelectrodes was performed in DI water and 10× PBS at room temperature (Fig. 8), revealing ideal measurement frequencies of 1 kHz for DI water and 1 MHz for 10× PBS. Baseline impedance magnitudes were 1.77 MΩ at 1 kHz for DI water and 803 Ω at 1 MHz

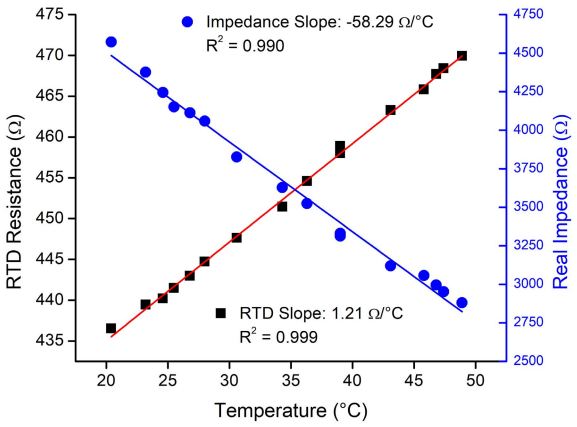

Fig. 6. Real impedance at 100 kHz and RTD resistance compared to thermocouple measurements. Impedance was roughly linear with temperature, with a temperature coefficient of resistance −58.29 Ω/°C and resolution of 0.02°C. This compared favorably to the RTD, which showed a temperature coefficient of resistance of 1.21 Ω/°C and a resolution of 0.08°C.

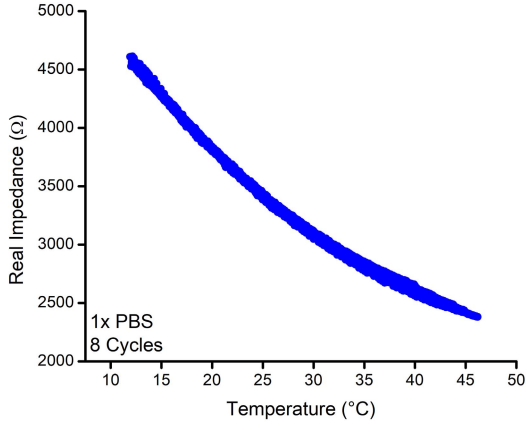

Fig. 7. Real impedance showed an inverse relationship with temperature, as measured using the platinum RTD on the same substrate. Minimal hysteresis was observed during repeated temperature cycles from 15 to 45°C.

for 10× PBS, compared to 5.55 kΩ at 100 kHz for 1× PBS. Temperature coefficients were found to be remarkably constant, even over a $>10^3$ change in solution resistance.

Electrode impedance and RTD resistance were monitored in flowing PBS at room temperature for 24 hours (Fig. 9). Both the RTD and the electrodes recorded ambient temperature fluctuations throughout the day. During the first three hours of measurement, the temperature as measured by the RTD increased approximately 2°C, a change which was not reflected in the real impedance measurement or the Sensirion temperature data. Between 3 and 24 hours, there was no detectable drift between the impedance measurement, the RTD resistance, and the Sensirion temperature data.

To examine drift, a sensor was immersed in 1× PBS and placed in an environmental chamber (EC0-A, Sun Electronic Systems Inc., Titusville, FL, USA) set to 37°C. After two hours of warmup time, over which time both the impedance-based temperature sensor and the RTD detected an increase from 21 to 37°C, the chamber maintained its temperature within the resolution of the chamber's thermocouple for the next 19 hours. Over this time, the electrode impedance dropped approximately 5.3% from its baseline value while the RTD resistance increased by 0.29%. Solution conductivity was measured before and after the experiment (A212, ThermoFisher, Waltham, MA, USA) to monitor evaporation, which detected an increase from 17.01 to 17.68 mS/cm. Correcting for this conductivity change results in only a 0.2°C error between temperature measurements using the electrodes versus using the platinum RTD (Fig. 10). This drift was not observed during tests at room temperature.

VI. Discussion

The experimental results demonstrate that electrochemical impedance is highly sensitive to changes in temperature. This effect was used to measure sub-degree temperature fluctuations at a higher resolution than platinum RTDs, which are considered the gold standard for fluid temperature transduction. High-speed and high precision measurement of changes in fluid temperature is useful in thermal anemometry; previous work has utilized the qualitative application of impedance-based temperature transduction to create highly sensitive liquid thermal flow sensors [20], [21].

Construction out of thin-film platinum on a Parylene C substrate renders this sensor flexible and resistant to corrosion. A flexible sensor is advantageous for packaging and will allow easy integration into the walls of shunts and catheters currently used in the clinic. However, flexing of the substrate may change the distance between electrodes, creating drift in impedance magnitude and preventing accurate temperature measurement. For accurate temperature transduction, electrode position and spacing should be fixed prior to calibration or baseline measurements. In addition, the use of Parylene C as a substrate material limits operation to temperatures below its glass transition temperature, which lies between 60 and 90°C [47], [48]. The current version of the sensor is designed for use between room temperature and 37°C, which do not exceed this temperature limit; future versions for industrial applications could be fabricated on borosilicate glass to avoid thermal degradation issues.

During 24 hours of continuous measurement at room temperature there was no significant drift in the electrode impedance compared to the RTD. However, when held at 37°C significant drift was observed in impedance measurements. This drift is most likely caused by increasing ionic concentration in the testing solution due to evaporation, as suggested by conductivity meter readings before and after testing. After correcting for changes in solution composition, drift remained below 0.2°C over a 21-hour period.

Future target applications for the temperature sensor described in this work will focus on temperature transduction *in vivo*. Variations in physiological fluid temperature can affect the calibration of biochemical sensors, so sensitive temperature measurement is useful to reduce noise and increase accuracy. Measuring the temperature of blood can also be useful for hemodynamic assessment and for calibration of blood pressure or flow sensors, and chronic measurement of CSF temperature can be used to monitor the efficacy of hydrocephalus treatment. Electrochemical impedance measurements

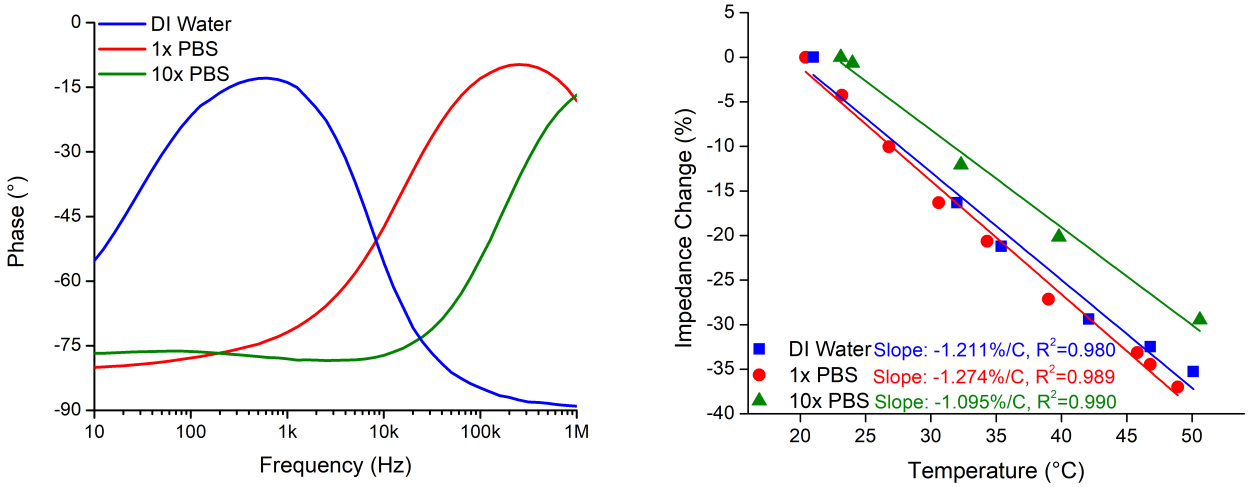

Fig. 8. Left: EIS showing the impedance phase across temperature sensing electrodes in DI water, 1× PBS, and 10×PBS. Higher ionic concentrations resulted in a shift of the ideal measurement frequency (where phase is minimized) towards higher frequencies. Right: Relative impedance compared to thermocouple measurements in DI water, 1× PBS, and 10× PBS. Temperature coefficients of real impedance in the resistive range stayed relatively constant despite a $>10^3$ change in solution resistance. Real impedance was measured at 1 kHz in DI water, 100 kHz in 1× PBS, and 1 MHz in 10× PBS.

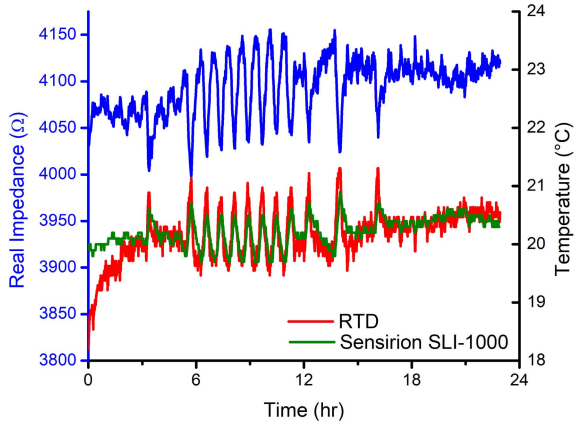

Fig. 9. Electrode impedance at 100 kHz in 1× PBS was measured once per minute for one day and compared to temperature as measured by the co-fabricated RTD. Real impedance and RTD temperature between 6 and 12 hours of measurement shows sub-degree changes in room temperature due to cycling of the air conditioning system of the laboratory.

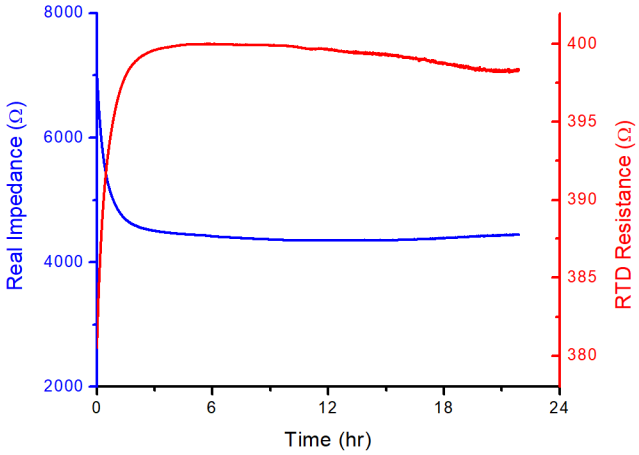

Fig. 10. Impedance and RTD resistance were measured during 21 hours of soaking in an environmental chamber set to 37°C. Over this time, temperature measurements by the impedance sensor drifted by approximately 0.2°C compared to temperature measurements by the platinum RTD.

are independent of the substrate and electrode material when measured at the appropriate frequency, since any surface effects are bypassed. Therefore, temperature measurement via electrochemical impedance can be extended to other rigid or flexible substrates and can be implemented in pre-existing medical devices such as pacemakers or continuous glucose monitors that already contain electrodes exposed to aqueous solution. Future studies will characterize the effects of biofouling on the measurement signal, and self-cleaning techniques such as cyclic voltammetry or electrolysis will be evaluated. Outside of the body, impedance-based temperature measurement has applications in microfluidics, diagnostic testing, and chemical processing, since these fields all require precise control of fluid temperature to manipulate reaction kinetics. The chemical inertness, biocompatibility, and corrosion resistance of both Parylene C and platinum make the sensor described in this work widely applicable throughout the biomedical and industrial spaces.

VII. Conclusion

A novel method of temperature transduction in aqueous solutions was explored using a polymer MEMS sensor. The sensor consisted of two exposed platinum electrodes embedded in a thin-film Parylene C substrate; temperature was transduced by measuring the electrochemical impedance between the electrodes at the frequency where phase was minimized. According to the Randles model, at this frequency, impedance will be dominated by solution resistance, which is highly temperature sensitive due to decreases in water's viscosity with increasing temperature. Experimental results showed that the sensor transduced fluid temperature with higher sensitivity and lower noise than a platinum RTD co-fabricated on the same

substrate; sensitivity was consistent over a wide range of ionic concentrations. This microfabricated polymer temperature sensor is flexible and corrosion resistant, lending itself to a wide range of applications in the chemical and biomedical fields. Future development will focus on practicality for chronic *in vivo* temperature transduction.

ACKNOWLEDGMENT

The authors would like to thank Dr. Brian Kim of Verily Life Sciences for his ideas and encouragement, Dr. Donghai Zhu of the Keck Photonics Lab for assistance with fabrication, and all the members of the Biomedical Microsystems Lab of USC for their help and support.

REFERENCES

[1] J. T. W. Kuo, L. Yu, and E. Meng, "Micromachined thermal flow sensors—A review," *Micromachines*, vol. 3, no. 3, pp. 550–573, Mar. 2012.

[2] E. Cabuz, J. Schwichtenberg, B. DeMers, E. Satren, A. Padmanabhan, and C. Cabuz, "MEMS-based flow controller for flow cytometry," presented at the Solid-State Sens., Actuators Microsyst. Workshop, Hilton Head, SC, USA, 2002.

[3] A. Cobo, R. Sheybani, and E. Meng, "MEMS: Enabled drug delivery systems," *Adv. Healthcare Mater.*, vol. 4, no. 7, pp. 969–982, 2015.

[4] L. Schöler *et al.*, "Monolithically integrated micro flow sensor for lab-on-chip applications," *Microelectron. Eng.*, vols. 78–79, pp. 164–170, Mar. 2005.

[5] A. S. Nezhad, M. Ghanbari, C. G. Agudelo, M. Packirisamy, R. B. Bhat, and A. Geitmann, "PDMS microcantilever-based flow sensor integration for lab-on-a-chip," *IEEE Sensors J.*, vol. 13, no. 2, pp. 601–609, Feb. 2013.

[6] Z.-S. Deng and J. Liu, "Blood perfusion-based model for characterizing the temperature fluctuation in living tissues," *Phys. A, Stat. Mech. Appl.*, vol. 300, nos. 3–4, pp. 521–530, Nov. 2001.

[7] M. D. Ginsberg, L. L. Sternau, M. Y. Globus, W. D. Dietrich, and R. Busto, "Therapeutic modulation of brain temperature: Relevance to ischemic brain injury.," *Cerebrovascular Brain Metabolism Rev.*, vol. 4, no. 3, pp. 189–225, 1992.

[8] R. Busto, W. D. Dietrich, M. Y.-T. Globus, I. Valdés, P. Scheinberg, and M. D. Ginsberg, "Small differences in intraischemic brain temperature critically determine the extent of ischemic neuronal injury," *J. Cerebral Blood Flow Metabolism*, vol. 7, no. 6, pp. 729–738, Dec. 1987.

[9] P. Childs, J. Greenwood, and C. Long, "Review of temperature measurement," *Rev. Sci. Instrum.*, vol. 71, no. 8, pp. 2959–2978, 2000.

[10] A. Tong, "Improving the accuracy of temperature measurements," *Sensor Rev.*, vol. 21, no. 3, pp. 193–198, 2001.

[11] S. O. Kapak, *Thermoelectric Effects in Metals: Thermocouples*. Saskatoon, SK, Canada: McGraw-Hill, 2001.

[12] F. Lacy, "Using nanometer platinum films as temperature sensors (constraints from experimental, mathematical, and finite-element analysis)," *IEEE Sensors J.*, vol. 9, no. 9, pp. 1111–1117, Sep. 2009.

[13] H.-M. Chuang, K.-B. Thei, S.-F. Tsai, and W.-C. Liu, "Temperature-dependent characteristics of polysilicon and diffused resistors," *IEEE Trans. Electron Devices*, vol. 50, no. 5, pp. 1413–1415, May 2003.

[14] A. Vanhoestenberghe and N. Donaldson, "Corrosion of silicon integrated circuits and lifetime predictions in implantable electronic devices," *J. Neural Eng.*, vol. 10, no. 3, Jun. 2013, Art. no. 031002.

[15] Y. Kanda, R. Aoshima, and A. Takada, "Blood compatibility of components and materials in silicon integrated circuits," *Electron. Lett.*, vol. 17, no. 16, pp. 558–559, Aug. 1981.

[16] H. Hämmerle, K. Kobuch, K. Kohler, W. Nisch, H. Sachs, and M. Stelzle, "Biostability of micro-photodiode arrays for subretinal implantation," *Biomaterials*, vol. 23, no. 3, pp. 797–804, Feb. 2002.

[17] S. B. Baumann, D. R. Wozny, S. K. Kelly, and F. M. Meno, "The electrical conductivity of human cerebrospinal fluid at body temperature," *IEEE Trans. Biomed. Eng.*, vol. 44, no. 3, pp. 220–223, Mar. 1997.

[18] L. H. J. Raijmakers, D. L. Danilov, J. P. M. van Lammeren, M. J. G. Lammers, and P. H. L. Notten, "Sensorless battery temperature measurements based on electrochemical impedance spectroscopy," *J. Power Sources*, vol. 247, pp. 539–544, Feb. 2014.

[19] R. R. Richardson, P. T. Ireland, and D. A. Howey, "Battery internal temperature estimation by combined impedance and surface temperature measurement," *J. Power Sources*, vol. 265, pp. 254–261, Nov. 2014.

[20] A. Baldwin, L. Yu, and E. Meng, "An electrochemical impedance-based thermal flow sensor for physiological fluids," *J. Microelectromech. Syst.*, vol. 25, no. 6, pp. 1015–1024, 2016.

[21] A. Baldwin, T. Hudson, and E. Meng, "A calorimetric flow sensor for ultra-low flow applications using electrochemical impedance," in *Proc. IEEE Micro Electro Mech. Syst. (MEMS)*, Jan. 2018, pp. 361–364.

[22] J. E. B. Randles, "Kinetics of rapid electrode reactions," *Discuss. Faraday Soc.*, vol. 1, pp. 11–19, Mar. 1947.

[23] J. O. M. Bochris and A. K. N. Reddy, *Modern Electrochemistry*, vol. 2. New York, NY, USA: Plenum Press, 1977.

[24] L. R. Faulkner and A. J. Bard, *Electrochemical Methods: Fundamentals and Applications*. Hoboken, NJ, USA: Wiley, 2002.

[25] D. R. Merrill, E. A. Jeffrey, and L. S. Jay, "The electrode—Materials and configurations," in *Essential Neuromodulation*. San Diego, CA, USA: Elsevier, 2011, pp. 107–152.

[26] J. Schefold and H.-M. Kühne, "Charge transfer and recombination kinetics at photoelectrodes: A quantitative evaluation of impedance measurements," *J. Electroanal. Chem. Interfacial Electrochem.*, vol. 300, no. 1, pp. 211–233, Feb. 1991.

[27] J. R. MacDonald, "Double layer capacitance and relaxation in electrolytes and solids," *Trans. Faraday Soc.*, vol. 66, pp. 943–958, 1970.

[28] A. A. Kornyshev, "Double-layer in ionic liquids: Paradigm change?" *J. Phys. Chem. B*, vol. 117, no. 44, p. 13946, 2007.

[29] M. Chen, Z. A. Goodwin, G. Feng, and A. A. Kornyshev, "On the temperature dependence of the double layer capacitance of ionic liquids," *J. Electroanal. Chem.*, vol. 819, pp. 347–358, Jun. 2017.

[30] R. A. Robinson and R. H. Stokes, *Electrolyte Solutions*. North Chelmsford, MA, USA: Courier Corporation, 2002.

[31] M. Berkowitz and W. Wan, "The limiting ionic conductivity of Na^+ and Cl^- ions in aqueous solutions: Molecular dynamics simulation," *J. Chem. Phys.*, vol. 86, no. 1, pp. 376–382, 1987.

[32] L. Onsager, "Theories of concentrated electrolytes," *Chem. Rev.*, vol. 13, no. 1, pp. 73–89, 1933.

[33] J. Daintith, *A Dictionary of Chemistry*, 6 ed. London, U.K.: Oxford Univ. Press, 2008.

[34] M. L. Huber *et al.*, "New international formulation for the viscosity of H_2O," *J. Phys. Chem. Reference Data*, vol. 38, no. 2, pp. 101–125, 2009.

[35] E. R. Nightingale, Jr, "Phenomenological theory of ion solvation. Effective radii of hydrated ions," *J. Phys. Chem.*, vol. 63, no. 9, pp. 1381–1387, 1959.

[36] G. M. Hochwald, A. Wald, J. DiMattio, and C. Malhan, "The effects of serum osmolarity on cerebrospinal fluid volume flow," *Life Sci.*, vol. 15, no. 7, pp. 1309–1316, Oct. 1974.

[37] C. D. Lee and E. Meng, "Mechanical properties of thin-film Parylene–metal–Parylene devices," *Frontiers Mech. Eng.*, vol. 1, p. 10, Sep. 2015.

[38] A. Cowley and B. Woodward, "A healthy future: Platinum in medical applications," *Platinum Met. Rev.*, vol. 55, no. 2, p. 98, Apr. 2011. Accessed: Jun. 9, 2019. [Online]. Available: https://www.ingentaconnect.com/content/matthey/pmr/2011/00000055/00000002/art00004

[39] S. Kuppusami and R. H. Oskouei, "Parylene coatings in medical devices and implants: A review," *Univ. J. Biomed. Eng.*, vol. 3, no. 3, pp. 9–14, 2015.

[40] B. J. Kim and E. Meng, "Micromachining of Parylene C for bioMEMS," *Polym. Adv. Technol.*, vol. 27, no. 5, pp. 564–576, May 2016.

[41] E. Meng, P.-Y. Li, and Y.-C. Tai, "Plasma removal of Parylene C," *J. Micromech. Microeng.*, vol. 18, no. 4, 2008, Art. no. 045004.

[42] N. Jackson, F. Stam, J. O'Brien, L. Kailas, A. Mathewson, and C. O'Murchu, "Crystallinity and mechanical effects from annealing Parylene thin films," *Thin Solid Films*, vol. 603, pp. 371–376, Mar. 2016.

[43] R. P. von Metzen and T. Stieglitz, "The effects of annealing on mechanical, chemical, and physical properties and structural stability of Parylene C," *Biomed. Microdevices*, vol. 15, no. 5, pp. 727–735, Oct. 2013.

[44] J. Ortigoza-Diaz *et al.*, "Techniques and considerations in the microfabrication of Parylene C microelectromechanical systems," *Micromachines*, vol. 9, no. 9, p. 422, Sep. 2018.

[45] B. J. Kim, E. P. Washabaugh, and E. Meng, "Annealing effects on flexible multi-layered Parylene-based sensors," in *Proc. IEEE 27th Int. Conf. Micro Electro Mech. Syst. (MEMS)*, Jan. 2014, pp. 825–828.

[46] C. A. Gutierrez, C. Lee, B. Kim, and E. Meng, "Epoxy-less packaging methods for electrical contact to Parylene-based flat flexible cables," in *Proc. 16th Int. Solid-State Sens., Actuators Microsyst. Conf. (TRANSDUCERS)*, Jun. 2011, pp. 2299–2302.
[47] H.-S. Noh, Y. Huang, and P. J. Hesketh, "Parylene micromolding, a rapid and low-cost fabrication method for Parylene microchannel," *Sens. Actuators B, Chem.*, vol. 102, no. 1, pp. 78–85, Sep. 2004.
[48] B. J. Kim and E. Meng, "Review of polymer MEMS micromachining," *J. Micromech. Microeng.*, vol. 26, no. 1, 2016, Art. no. 013001.

Alex Baldwin received the B.S. degree in electrical engineering from the University of Arkansas, Fayetteville, AR, USA, in 2013, and the M.S. and Ph.D. degrees in biomedical engineering from the University of Southern California (USC), in 2015 and 2018, respectively. His graduate and post-doctoral work focused on improving the treatment of hydrocephalus using chronically implantable sensors and remote patient monitoring. He is currently developing novel neurostimulation-based therapies at Niche Biomedical Inc. His research interests include bioelectronic medicine, chronically implantable medical device, and biomedical sensors. He was a recipient of the USC Viterbi Fellowship and the Alfred E. Mann Institute Fellowship.

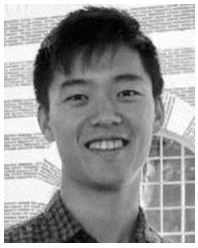

Eugene Yoon received the B.S. degree in chemical and biomolecular engineering from the Johns Hopkins University, Baltimore, in 2015, and the M.S. degree in biomedical engineering from the University of Southern California (USC), Los Angeles, in 2017. He is currently pursuing the Ph.D. degree in biomedical engineering with USC, where his research is focused on bioMEMS sensors and implantable microdevices.

Trevor Hudson received the B.S. degree in biomedical engineering from Rice University, in 2014, and the M.S. degree in biomedical engineering from the University of Southern California (USC), in 2016. He is currently pursuing the Ph.D. degree with USC, where he researches implantable impedimetric sensors and polymer micromachining.

Ellis Meng (M'02–SM'09–F'16) received the B.S. degree in engineering and applied science and the M.S. and Ph.D. degrees in electrical engineering from the California Institute of Technology (Caltech), Pasadena, in 1997, 1998, and 2003, respectively. She is currently a Professor of biomedical engineering and the Vice Dean of Technology Innovation and Entrepreneurship of the Viterbi School of Engineering, University of Southern California, Los Angeles, where she has been, since 2004. She also holds a joint appointment in the Ming Hsieh Department of Electrical and Computer Engineering. Her research interests include bioMEMS, implantable biomedical microdevices, microfluidics, multimodality integrated microsystems, and packaging. She is also a Fellow of ASME, BMES, NAI, and AIMBE. She held the Viterbi Early Career Chair at the Viterbi School of Engineering and was the Department Chair, from 2015 to 2018. She is also an Inaugural Holder of a Gabilan Distinguished Professorship in Science and Engineering. Her honors include the NSF Career award, Wallace H. Coulter Foundation Early Career Award, 2009 TR35 Young Innovator Under 35, Viterbi Early Career Chair, ASEE Curtis W. McGraw Research Award, and 2018 IEEE Engineering in Medicine and Biology Society Technical Achievement Award.